Impact of faults on the efficiency curve of flat plate solar collectors: a numerical analysis

Gaëlle Faure, Mathieu Vallée, Cédric Paulus, Tuan Quoc Tran

Version of Record: https://www.sciencedirect.com/science/article/pii/S0959652619316464
Manuscript_406f60bca47784d684302b813821502f

Word count: 7539

Impact of faults on the efficiency curve of flat plate solar collectors: a numerical analysis

Gaëlle Faure[1,*], Mathieu Vallée[1], Cédric Paulus[1], Tuan Quoc Tran[2]

1. Univ. Grenoble Alpes, CEA, LITEN, DTBH, LSED, F-38000 Grenoble, France
2. Univ. Grenoble Alpes, CEA, LITEN, DTS, LSEI, F-38000 Grenoble, France

Abstract: Thermal solar energy is one of the promising cleaner ways to produce heat. In particular, large scale solar thermal systems (LSTS) can produce low-cost heat for use in district heating networks or industrial processes. However, return on investment is based to long-term reliable operation, and automatically detecting dysfunctions is desirable in these systems. Existing fault detection and diagnosis methods are applicable on many components in such a system, but the impact of faults on solar collectors received little attention. In this paper, the impact of three different faults on solar collectors is analyzed: the « transparent cover failure » fault, the « opacification » fault and the « insulation degradation » fault. To perform this analysis, a numerical model covering both normal and faulty operation is proposed. The model can be tailored to a given solar collector based only on datasheet parameters, and the experimental validation shows a good accuracy, without any calibration, both in normal and faulty operation. This model is used to study in detail the impact of the three studied faults on the solar collector efficiency curve. The results show that some assumptions made in previous work can be challenged, while other are validated for a wider range of conditions thanks to the model presented in this paper.

Keywords: thermal solar; fault; flat plate solar collector; fault effect.

1 INTRODUCTION

A transition towards a low-carbon energy system is essential to face the climate change concern as energy sector is responsible for the two thirds of GES world emissions [1]. Heat and cold needs are significant (46 % in European Union in 2014 [2]) and are today mainly covered by non-renewable sources. Thermal solar energy is one of the promising cleaner ways to produce them.

As all industrial processes, thermal solar systems are subject to dysfunctions. As key element of these installations, a failure of the solar collector has a significant impact on the production of the installation. The performance of this component is traditionally characterized by the three normative efficiency coefficients η_0, a_1 and a_2 which determine the efficiency curve of a solar collector(ISO 9806:2014 ; [3]). A modification of these coefficients strongly affect the solar production as demonstrated by Hellstrom *et al.*[4], who analyzed the impact of the modification of a solar collector on its steady-state performance and its annual production, and Rehman *et al.*[5] in their study of the influence of failures on a solar heating system. There are only few works about analysing the influence of a solar collector fault on the efficiency of this component whereas it is more common in other areas such as the work of Bun [6] who compared the influence of different dysfunctions on the I-V curve of PV panels. The purpose of this paper is therefore to assess the relationship between faults and the efficiency curve of a solar collector.

* Corresponding author. Email: research@gaellefaure.fr

Data to analyse the impact of a fault on the behaviour of a system can be produced either by experimental or simulation means. However obtaining experimental data of a faulty system is in general not possible or limited to one specific fault and one specific system. On the other hand, a numerical model is flexible and allows a deep understanding of the system both in faulty and normal modes. In this paper, a numerical study on the impact of three solar collector faults on the efficiency coefficients is developed:

- the « transparent cover failure » fault which gathers two main failures : a broken glass cover and the tearing of the FEP foil if any ;
- the « opacification » fault related to the opacification of the glass cover ;
- the « insulation degradation » fault linked to a decrease of the thermal insulation ability of the back insulation.

To achieve this goal, a model of a flat-plate solar thermal collector is developed. Versions of this model are derived to reproduce the behavior of a collector affected by the three presented faults. Experimental data enable a validation of these models for some cases. They are then used to simulate the three faults with different severity and to obtain the corresponding steady-state efficiency coefficients.

The organization of this paper is as follows: section 2 presents a state of the art about solar collector faults and their impact on its efficiency. The models of the solar collector in normal and faulty operation are then detailed in section 3. Section 4 presents the experimental validation of the different models. Finally section 5 provides an analysis of the faults impact on the efficiency coefficients, completed by a comparison with the literature. Section 6 concludes this paper.

NOMENCLATURE

LATIN SYMBOLS

A	Solar collector area	m²
a_1	Linear thermal losses coefficient	W/(m².K)
a_2	Quadratic thermal losses coefficient	W/(m².K²)
C	Heat capacity	J/K
cp	Specific heat capacity	J/(kg.K)
$f(t)$	Function representing a fault	-
f_i	Element of the function $f(t)$	-
F'	Collector efficiency factor	-
g	Relationships between inputs and outputs of a system	-
G	Total solar radiation reaching a solar collector	W/m²
h	Heat transfer coefficient	W/K
P	Thermal power produced by a solar collector	W
s	Severity of a fault	-
t	Time	s
T_a	Ambient temperature	K
T_{in}	Inlet fluid temperature	K
T_m	Mean solar collector temperature	(K.m²)/W
T_m^*	Reduced temperature	-
$U(t)$	Vector of the measured input signals	-
$Y(t)$	Vector of the measured output signals	-

GREEK SYMBOLS

α	Optical absorption coefficient	-
Δ	Difference	-
η_0	Optical efficiency	-
η_{std}	Steady-state efficiency	-
θ	Vector of parameters of the system	-
λ	Thermal conductivity	W/(m².K)
ρ	Optical reflectance	-
τ	Optical transmittance	-
$(\tau\alpha)$	Transmittance-absorptance product	-
ϕ	Radiation flux	W

SUBSCRIPTS

c	Related to glass cover
dif	Related to diffuse solar radiation
dir	Related to direct solar radiation
eq	Related to an equivalent feature
i, j, k	Element of a vector
in	Related to an inlet flux
$isol$	Related to « insulation degradation » fault
opa	Related to « opacification » fault
out	Related to an outlet flux
ref	Related to a reference feature
t	Related to FEP foil

2 FAULTS AND THEIR IMPACT ON SOLAR COLLECTOR EFFICIENCY: STATE-OF-THE ART

A comprehensive study of faults affecting solar collectors can be found in previous work by the authors of the present study [7]. One significant conclusion of this work is that almost all these faults directly affect the amount of energy produced by the solar collector.

Solar collector performance is generally characterized by its steady-state efficiency curve. This curve links the steady-state efficiency of the collector η_0 to total solar irradiation G, ambient temperature T_a and mean solar collector temperature T_m. The relation is defined by norm ISO 9806:2014 [3] as a second-order polynomial with three coefficients (see (1)) called the efficiency coefficients: the optical efficiency η_0 without unit, the thermal losses linear coefficient a_1 in W/(m².K)and the thermal losses quadratic coefficient a_2 in W/(m².K²).

$$\eta_{std} = \frac{P}{A.G} == \boldsymbol{\eta_0} - \boldsymbol{a_1} T_m^* - \boldsymbol{a_2} G {T_m^*}^2 \quad (1)$$

In (1), $T_m^* = \frac{T_m - T_a}{G}$ is the reduced temperature in (K.m²)/W. This variable captures the main effects of the boundary conditions on the system [8].

Tagliafico *et al.* [9] and Schnieders [10] reviewed and compared physics-based thermal solar collectors models. They proposed to classify the existing models by complexity: from steady-state to lumped constants, discretized along the fluid and finally CFD (Computational Fluid Dynamics) models. They showed that the more complex the model is the more accurate but also the more time and computational consuming.

Solar collector models reproducing faulty operation are often used to validate fault detection and diagnosis methods [11–13]. The authors model the faults by a 1-node lumped capacity model based on the equation (1). The faults are reproduced by a modification of efficiency coefficients however they cannot always easily be linked to physical phenomena, in particular the thermal losses coefficients a_1 and a_2. Several authors developed models with more nodes, which enable a parameterization with physical features and are more accurate. Matuska *et al.* [14] developed a small software called Kollektor 2.2, which allows the design of flat plate thermal solar collectors. The tool does a detailed calculation the steady-state heat transfers between the different elements of the collector and deduces the normative efficiency curves. The model comprises seven thermal nodes and is experimentally validated. Zima and Dziewa [15] proposed a 5xN-nodes model and a special care was taken in the choice of the number of nodes along the fluid. Eventually a quite high value was chosen (96) and the validation showed a good reproduction of the steady-state as well as the transient-state behaviors of a solar collector. Hamed *et al.*[16] developed a non discretized 4-nodes model to analyze the energy and the exergy of a flat-plate solar thermal collector in transient-state. They assume a uniform repartition of the fluid in the solar collector. Herrero Lopez *et al*. [17] developed and compared two solar collector models: a simplified 1 node-lumped capacity model based on the ISO 9806:2014 norm and a more detailed 5 nodes-model. The validation with transient-state experimental data shows a better accuracy of the detailed model. Kamiński and Krzyżyński [18] proposed two ways to simulate a solar thermal collector: a discretized 3xN-nodes model and a CFD model. In the discretized model, the absorber plate presents a 2D discretization to better take account the repartition of the temperature. The validation with short-term and long-term experimental data demonstrates that the CFD model is more appropriate for a geometrical optimization. In the other cases the discretized model shows a better compromise between computational time and accuracy. The presented studies do not use the models to reproduce the faulty operation of a solar collector. And to the best of our knowledge, such study with a detailed model does not exist.

There are currently no existing studies about the impact of a fault on the efficiency curve of a thermal solar collector. The most similar studies concern the impact of improvements on a solar collector and they only cover one particular case with one set of efficiency coefficients. Bava and Furbo [19] compared experimentally and numerically the efficiency of two single-glazed thermal solar collectors, one with and one without FEP foil. Hellstrom *et al.* [4] analyse impact of several improvements of the solar collector on energy produced and efficiency coefficients. They especially consider the addition of a FEP foil and the replacement of the cover glass by an antireflective-coated low-iron glass. Bellos *et al.* [20] simulated a single-cover flat plate collector with a CFD model and tested the impact of several constructions on the solar collector steady-state efficiency. Among them, a version without transparent cover is proposed and the results showed a slight increase of η_0 and a strong rise of the thermal losses. Vejen *et al.* [21] described a numerical and experimental procedure to improve the performances of a flat-plate solar collector for medium and large solar heating systems. They showed that the addition of an antireflection coating increased the optical efficiency η_0 of the solar collector. They also tested the impact of three different insulation materials with different thermal conductivities. The present study covers a more complete study of various faults, so that our results extend all these previous works.

3 DESCRIPTION OF THE SOLAR COLLECTOR MODELS

Based on the review of existing models and previous literature, a new solar collector model was developed to meet the requirements of this study, i.e. a model enabling a simple collector fault modeling. This model comprises several thermal nodes in order to be parameterized with physical and measurable parameters. In this part, the flat plate solar collector model in normal operation is presented. Then the required modifications of the model to properly reproduce the three studied faults are summarized.

3.1 NORMAL OPERATION MODEL

A flat plate solar collector is made of different components: one or two cover glasses potentially completed with a Fluorinated Ethylene Propylene (FEP) foil, an absorber plate, pipes in which the heating fluid circulates, back and edge insulation and housing. Our model is based on a simplified representation of the collector (Fig. 1) in which insulation and housing are grouped in one component. In the figure, the bond with the pipes is intentionally bigger than in reality.

Each component is considered as a lumped capacitance and exchanges heat with its neighbors by means of convection, conduction and long-wave (LW) radiations. Fig. 1 summarizes the different heat exchanges between the different components accounted for in the present study. Each temperature node has an associated lumped capacitance$C$, which is not represented for the sake of clarity. Solar radiation is treated apart with the help of optical properties of the components. The absorber plate is discretized to take into account the fin effect in the plate, which has a strong impact on collector efficiency [22]. Fin effect is the result of the uniform heating of the absorber by solar radiation in one side and the cooling localized at the bond with pipe in the other side resulting in a non-uniform distribution of the plate temperature.

The thermal balance in each node of temperature T and lumped capacitance C is given by the global equation (2) below, where $\phi_{i,in}$ and $\phi_{j,out}$ are the long-wave and solar radiations which respectively enter or leave the node, h_k are the thermal heat transfer coefficients corresponding to convection and conduction with the nodes nearby affected of temperatures T_k.

$$C\frac{dT}{dt} = \sum_i \phi_{i,in} - \sum_j \phi_{j,out} + \sum_k h_k(T - T_k) \qquad (2)$$

All the heat transfer coefficients h_k are calculated using the correlations used by Matuska *et al.* in the Kolektor handbook [14]:

- Heat transfer by wind convection from glazing to ambient: McAdams correlation [23];
- Nusselt number for natural convection in closed gas layer between absorber and FEP foil, and between FEP foil and glazing: A1 correlation from Matuska *et al.* [14];
- Nusselt number for natural convection in closed gas layer between absorber and back insulation: correlation from Arnold *et al.* [24];
- Nusselt number for forced convection in pipes: Shah correlation [25] for laminar flow, Colburn correlation [26] for turbulent flow.

Details of these correlations are available in the Kolektor handbook [14], as well as in the PhD thesis related to this work [27] (in French).

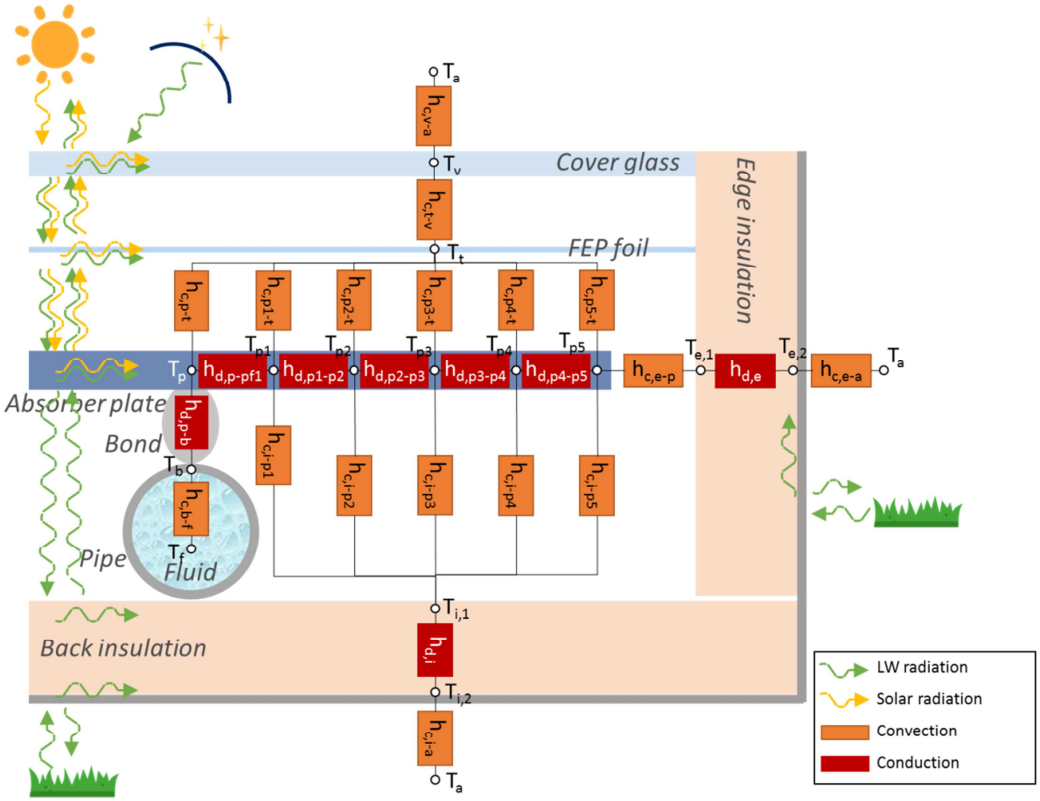

Fig. 1. Thermal-electric representation of the flat plate solar collector model: example of a collector with a FEP foil.

To facilitate its implementation, a modular approach based on the Modelica language is applied to the modeling of the solar collector, i.e. each component and associated thermal node is a module, as well as each heat exchange. The final model has around 50 parameters including geometrical values and thermal and optical properties of each component.

3.2 « TRANSPARENT COVER FAILURE » FAULT MODELING

This fault gathered two failures linked to the transparent cover:

- the breaking of one or more cover glasses: this failure is generally due to extreme weather conditions or bad choice of material [28],
- the tearing of the FEP foil if there is any. This foil is used in some solar collectors to replace a heavy second glass cover. Its tearing is generally due to a bad installation or ageing.

Both failures lead to a strong increase of the thermal losses of the solar collector as well as a small rise of the amount of transmitted solar radiation to the absorber plate. They strongly affect the structure of the solar collector, so variant of the solar collector model are built to represent them. The Fig. 2 shows the developed models for a solar collector with one cover glass and a FEP foil.

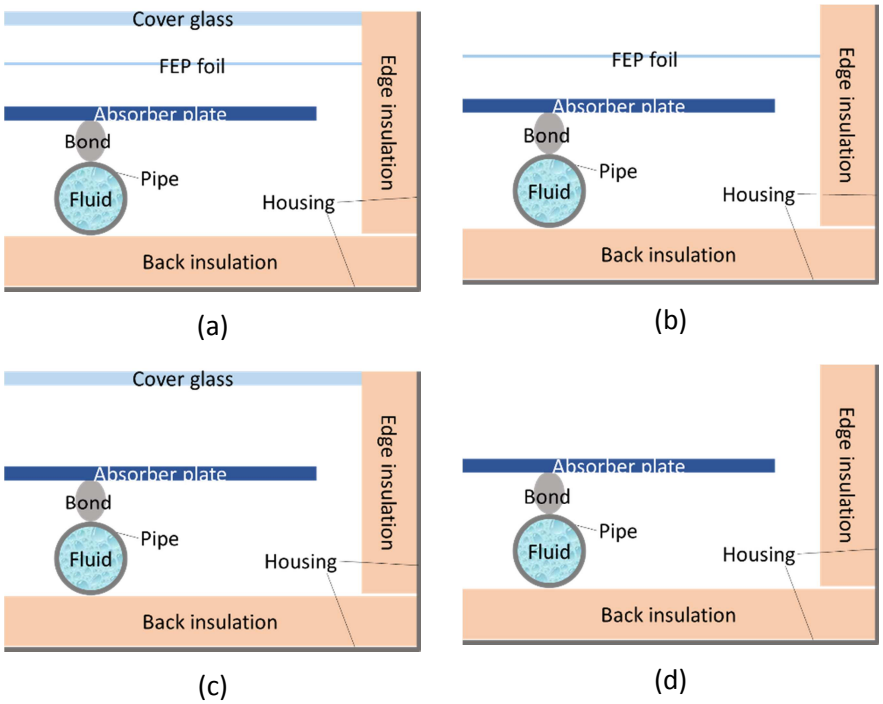

Fig. 2. The models of the different cases of the « transparent cover failure » fault for a solar collector with one cover glass and a FEP foil: (a) no fault, (b) without glass cover denoted "withoutGlass",(c) without FEP foil denoted "withoutFEP", (d) without any remaining transparent cover denoted "withoutCovers".

3.3 « OPACIFICATION » FAULT MODELING

Opacification of the solar collector is one of the causes of a decrease of the energy production of solar collectors. Opacification can be due to dust or air pollution. It affects the cover glass by lowering its transparency, i.e. its capacity to transmit the light. This capacity is described by the transmittance τ of the glass, which is an optical characteristic of the component. In the collector model, direct and diffuse solar radiations were treated separately, and so direct transmittance τ_{dir} and diffuse transmittance τ_{dif} coefficients are defined.

From the mathematical point of view, the nomenclature developed by Iserman [29] is used. Let us consider a process modeled by (3) in which $U(t)$ represents the measured input signals, $Y(t)$ the measured output signals, g the relationships between inputs and outputs and θ the parameters of the model.

$$Y(t) = g[U(t), \theta] \tag{3}$$

Let $f(t)$ be the function representing the « opacification » fault (referred as 'opa') and its time evolution. Its effect on the system can be modeled by (4):

$$Y(t) = g[U(t), (1 - f(t)).\theta] \tag{4}$$

$f(t)$ is described by (5):

$$f(t) = \begin{cases} f_i = s_{opa} \text{ for } \theta_i \in \{\tau_{dif}, \tau_{dir}\} \\ f_i = 0 \text{ otherwise} \end{cases} \tag{5}$$

with $s_{opa} \in [0,1]$, a constant representing the severity of the « opacification » fault. For $s_{opa} = 0$, $f_i = 0$ for $\theta_i \in \{\tau_{dif}, \tau_{dir}\}$ and $(1 - f_i)\tau_{dif/dir} = \tau_{dif/dir}$, so the transmittances stay unchanged: there is no fault. On the contrary, for $s_{opa} = 1$, $f_i = 1$ for $\theta_i \in \{\tau_{dif}, \tau_{dir}\}$ and $(1 - f_i)\tau_{dif/dir} = 0$: the cover glass is completely opaque to solar radiation. Between these extreme values, the severity

of the « opacification » fault s_{opa} represents the diminution of the two transmittances compared to the non-faulty ones.

3.4 « INSULATION DEGRADATION » FAULT MODELING

The degradation of the insulation of a solar collector can be due to the humidification of this insulation by the rain following a bad conception or installation. Insulation degassing can also occur after a wrong material choice during the design of the collector. In all case, the main effect of this fault is a decrease of the ability of the solar collector to limit heat transfer with external environment and so a smaller production.

In this study, only the case of the humidification of the insulation is treated. This fault directly affects the conductivity of the insulation λ_{isol}. As water is added to the material, the heat capacity of the insulation cp_{isol} is also modified. Both are increased. Upper bonds of these parameters are given by literature values for saturated water insulation materials typically used in solar collector design (mineral wool ; [30,31]). The ratios between normal and saturated values are respectively around 16 and 4. The « insulation degradation » is therefore modeled on the same principle as « opacification » fault with $f(t)$ defined by the equation (6).

$$f(t) = \begin{cases} f_i = -15 \times s_{isol} \text{for } \theta_i = \lambda_{isol} \\ f_i = -3 \times s_{isol} \text{for } \theta_i = cp_{isol} \\ f_i = 0 \text{ otherwise} \end{cases} \quad (6)$$

with $s_{isol} \in [0,1]$, a constant representing the severity of the « insulation degradation » fault. For $s_{isol} = 0$, $f_i = 0$ for $\theta_i \in \{\lambda_{isol}, cp_{isol}\}$, so in the same way as for the « opacification » fault there is no modification of the parameters and thus no fault. For $s_{isol} = 1$, $f_i = -15$ for $\theta_i = \lambda_{isol}$ and $f_i = -3$ for $\theta_i = cp_{isol}$, so we have $(1 - f_i)\lambda_{isol} = 16.\lambda_{isol}$ and $(1 - f_i)cp_{isol} = 4.cp_{isol}$: when the fault is maximal, the conductivity of the insulation λ_{isol} is multiplied by 16 and the heat capacity cp_{isol} is multiplied by 4. The two parameters are simultaneously modified and so the severity of the « insulation degradation » fault s_{isol} represents the extent of the increasing of the two parameters, knowing the possible range of their values.

4 EXPERIMENTAL VALIDATION IN NORMAL AND FAULTY OPERATION

In this section the model of a normal behavior as well as the models for the faulty behaviors presented in section 3 are validated using experimental measurements.

4.1 TEST PROCEDURE

Norm ISO 9806:2014 [3] defines the normative test plan for obtaining the efficiency coefficients. It consists in obtaining several steady-state operating points, by varying only the fluid inlet temperature. A steady state is defined by a variation of all the variables below the values indicated in Tab. 1. Thus the evolution of the steady-state efficiency η_{std} as a function of the reduced temperature T_m^* can be drawn. Knowing the shape of the link between the two variables (see (1)), a quadratic regression allows to determine the three efficiency coefficients η_0, a_1 and a_2.

Tab. 1. Maximal authorized variation of the main variables during the experimental record of one steady-state point according to the ISO 9806:2014 norm [3].

Feature	Symbol	Maximal variation
Total solar radiation	G	• Spatial: ± 15% • Temporal: ± 50 W/m²
Ambient temperature	T_a	± 1.5 K
Wind speed	v_{wind}	± 1 m/s
Mass flow	$\dot{m}$	± 1%

Inlet temperature	T_{in}	± 0.1 K
Outlet temperature	T_{out}	± 0.5 K

4.2 EXPERIMENTAL TEST STAND AND TESTED SOLAR COLLECTOR

Our indoor test stand is presented in Fig. 3 and Fig. 4. It is laboratory equipment for the testing of solar thermal collectors as well as PV-modules. The system consists of the steady-state solar simulator, including the lamp field and the artificial sky, as well as the collector test platform including the X-Y-scanner and the ventilation unit (see Fig. 4). The test stand is completed by the switching cabinets and all control means (e.g. software). It enables the measurement of the steady-state efficiency of solar thermal collectors according to ISO 9806:2014 norm [3] with artificial solar radiation.

Fig. 3. Indoor test stand for solar thermal collectors.

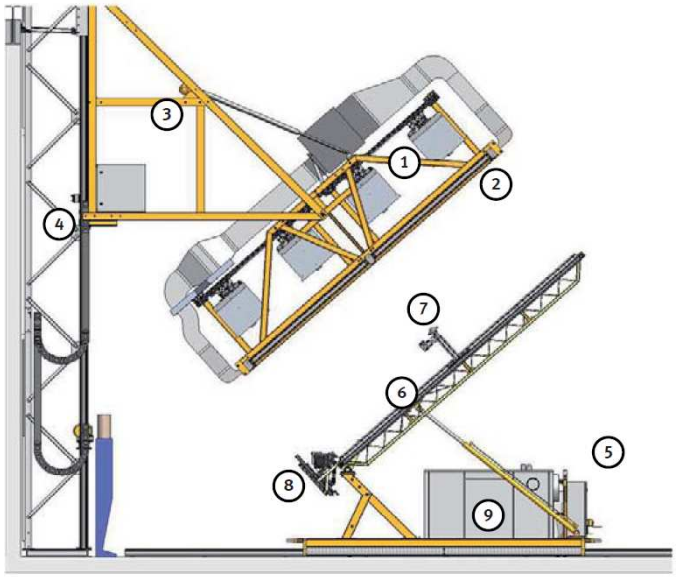

1	Lamp field
2	Artificial sky
3	Vertical carriage for the height adjustment of the lamp rig
4	Vertical support
5	Collector test platform
6	Collector support
7	X-Y-scanner
8	Ventilation unit
9	Thermostat

Fig. 4. Main components of the indoor test stand for solar thermal collectors.

The tested solar collector is a typical single glazed solar collector for domestic applications. The Fig. 5 presents a cross-section view of the tested solar collector. Its main features are summarized in Tab. 2.

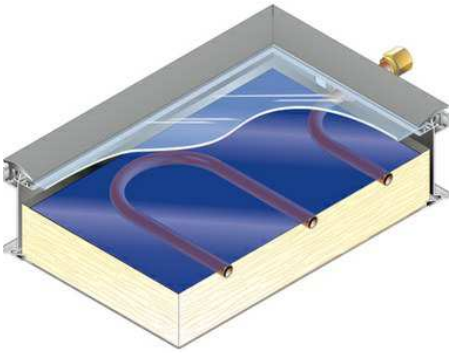

Fig. 5. Cross-section view of the Weishaupt solar collector [32].

Tab. 2. Main characteristics of the Weishaupt solar collector [32].

Manufacturer	Weishaupt
Model	WTS F1 – type K1
Aperture area	2.32 m²
Gross area	2.51 m²
Transparent cover	Single glazed: 3.2 mm tempered glass without antireflection coating
Absorber	0.5 mm aluminium sheet + selective coating of MIROTHERM type
Thermal insulation	50 mm back: mineral wool
Pipes	Meander : copper pipes, diameter 12 mm. Total length : 24 m
Housing	Aluminium

4.3 VALIDATION RESULTS

The experimental test stand is first used to characterize the normal steady-state efficiency of the solar collector. As a second step, the steady-state efficiency of the solar collector under the following faults is also characterized:

- « Transparent cover failure » fault: the cover glass of the solar collector is removed.
- « Opacification » fault: commercial adhesive film for windows, used to lower the solar radiation, was applied on the cover glass of the solar collector. Two different films (denoted opa1 and opa2) were used.
- « Insulation degradation » fault: the back of the housing as well as the back insulation were removed.

Please note that no variation of the incidence angle of the solar radiation was tested.

In parallel, the experimental procedure of ISO 9806:2014 norm [3]corresponding to the normal and faulty cases described above is numerically reproduced. The parameters of the numerical model are defined using only the manufacturer datasheet and usual material parameters.

Fig. 6 compares the efficiency curves obtained with experimental measurements and simulation. These results show that the model is generally very close to measurements both in normal and faulty behavior, with different modification of efficiency curves for each fault. As can be seen on Fig. 6.a the measurements in normal operation are in good accordance with the efficiency coefficients provided by the manufacturer datasheet. Simulated efficiency is better since the model represents an ideal solar collector and does not take into account elements such as, for instance, thermal bridges and other manufacturing defects. The « transparent cover failure » fault shows a larger gap between measures and simulation (see Fig. 6.b): the mean difference between measured and simulated efficiency is 0.09.The main explanation for this gap is a too simplified modeling of the convective heat exchange between the top of the solar collector and the ambient air, which is predominant in this case. However the general trend is respected. Fig. 6.c and Fig. 6.d show that in the case of the « opacification » and « insulation degradation » faults there is no significant difference between measure and simulation. No parameter identification was performed: manufacturer data sheet and usual material properties gave sufficiently accurate results.

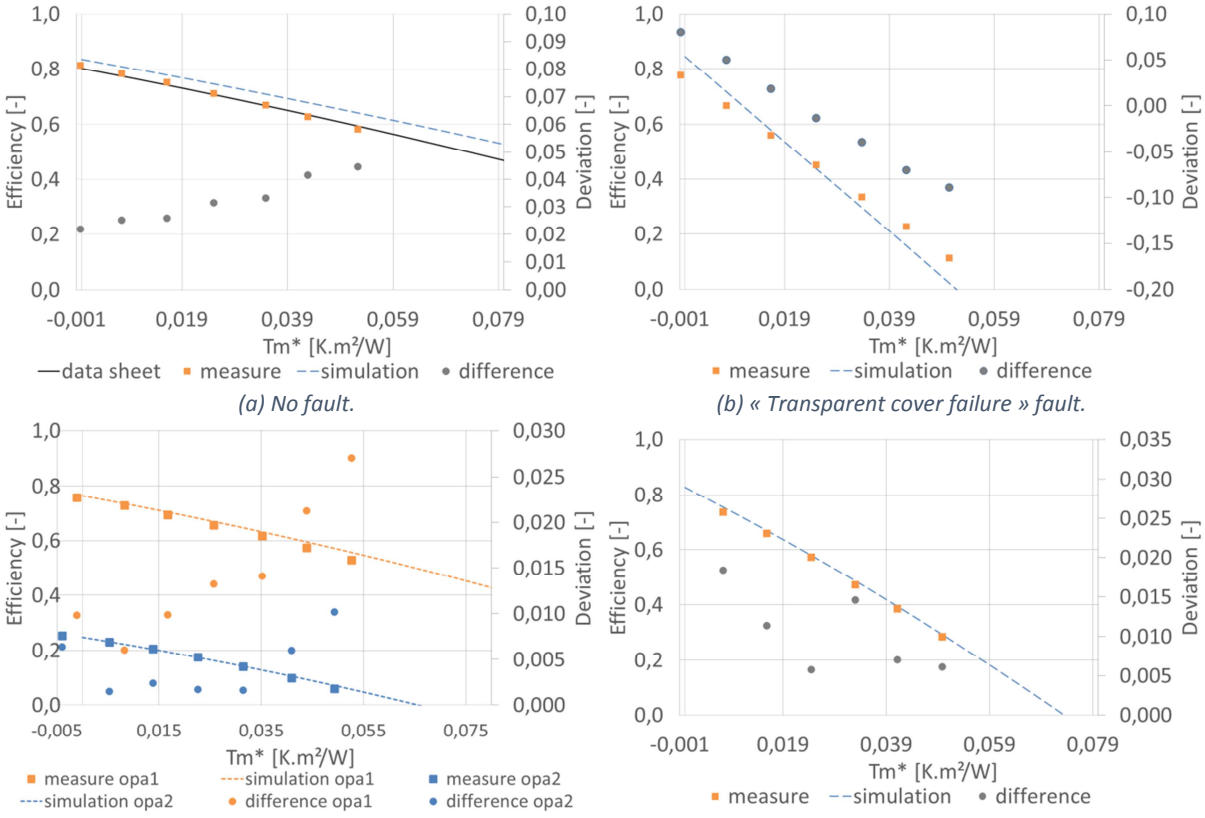

(a) No fault. *(b) « Transparent cover failure » fault.*

(c) « Opacification » fault. *(d) « Insulation degradation » fault.*

Fig. 6. Experimental and simulated efficiency curves as well as deviation between these curves for the different tests for a total incident radiation of 1000 W/m².

5 IMPACT OF FAULTS ON THE SOLAR COLLECTOR EFFICIENCY CURVE

In this section, the developed and validated numerical models were used to analyse the impact of the three faults on the solar collector efficiency curve. For each fault, efficiency curves are obtained with the same procedure as the one used for the validation. Several severities are tested to analyse their impact on the results. Finally, these results are compared to the limited data available in the literature. The configuration of the model corresponds to a typical flat plate solar collector designed for large solar thermal installations: the edge insulation is reinforced and there is a FEP foil in addition to the cover glass.

5.1 « TRANSPARENT COVER FAILURE » FAULT

According to the chosen solar collector design, the different cases of this fault are those described in the Fig. 2.

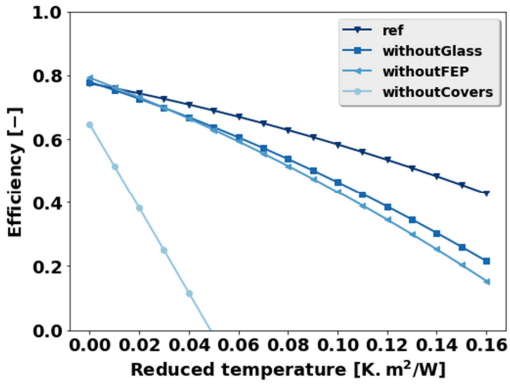

Fig. 7. Efficiency curves of a single collector for the different cases of the "transparent cover failure" fault for a direct solar radiation of 1000 W/m² (no diffuse radiation).

Tab. 3. Efficiency coefficients for the different cases of the "transparent cover failure" fault.

case	reference	*withoutGlass*	*withoutFEP*	*withoutCovers*
η_0	0.774	0.779	0.792	0.647
a_1	1.49	2.53	2.93	13.21
a_2	0.004	0.006	0.007	0.001

Fig. 7 and Tab. 3 show the results of the study for the different cases. The efficiency curves are typical of double-glazed (ref), single-glazed (*withoutGlass* and *withoutFEP*) and unglazed (*withoutCovers*) solar collectors. The curves for the cases *withoutGlass* and *withoutFEP* are slightly higher than the one of the non-faulty solar collector for a reduced temperature T_m^* of 0, then they decrease faster. Indeed, removing the glass cover or the FEP foil increases the fraction of incident solar radiation on the absorber plate. This gain is particularly visible when the mean temperature of the fluid crossing over the solar collector is equal to the ambient temperature ($\mathrm{T_m^*} = 0$, e.g. no thermal losses). This point corresponds to the efficiency coefficient η_0 of the efficiency equation (1), also called optical efficiency. This coefficient is actually slightly higher for the cases *withoutGlass* and *withoutFEP* on the Tab. 3. With only one transparent cover, on the other hand, more thermal losses are expected and indeed the coefficients a_1 and $a_2$increase in Tab. 3.

The curve of the case *withoutCovers* is much lower than the others and its shape is almost linear. The removal of the whole transparent cover suppresses the motionless air space above the absorber plate which enables a good insulation of the upper surface of this one. Thermal losses are therefore much higher. They are essentially due to the forced convection between absorber and the ambient air, which is proportional to the temperature difference of these two elements [14,22]. That explains the linear shape of the curve and a huge increase of the linear coefficient of thermal losses a_1 while a_2 decreases. On the contrary of the precedent cases one can however observe a reduction of the optical efficiencyη_0. Indeed, the temperature of the absorber plate is not uniform, due to the well-known fin effect [18,22], and in particular a significant part of the plate is hotter than the fluid. Thus, even at $\mathrm{T_m^*} = 0$, there are thermal losses, which are more important when there is no transparent cover.

Our results can be compared with two types of studies in the literature: collectors with and without FEP foil which correspond to our reference and *withoutFEP* cases and single-glazed and unglazed collectors which correspond to *withoutFEP* and *withoutCovers* cases. Bava *et al.* [22] as well as Hellstrom *et al.* [4] both presented studies comparing collectors with and without FEP foil, which correspond to our reference and *withoutFEP* cases. Tab. 4 thus presents their results together with the ones obtained in the present study: this show that all results are consistent even if the increase of a_1 is much more pronounced in our case. However a lack of information about parameterization and characteristics of the model of these studies do not allow concluding about this difference.

Tab. 4. Comparison of efficiency coefficients of the present study with literature for the ref and withoutFEP cases.

	Present study		(Bava *et al.*, 2015) [33]		(Hellstrom *et al.*, 2003) [4]	
	ref	*withoutFEP*	ref	*withoutFEP*	ref	*withoutFEP*
η_0	0.774	0.792	0.816	0.85	0.788	0.809
$\Delta\eta_0$		0.02		0.03		0.02
a_1	1.49	2.93	2.418	3.095	2.69	3.42
Δa_1		1.44		0.68		0.73
a_2	0.004	0.007	0.0085	0.0111	0.0082	0.0113
Δa_2		0.003		0.0026		0.0031

In a different kind of study, Bellos *et al.*[20] obtained with CFD simulations efficiency coefficients of a solar collector with and without a glass cover. This corresponds to our *withoutFEP* and *withoutCovers* cases. The present results can also be compared to those of the experimental validation of section 4. Tab. 5 sums up all the values. Since Bellos *et al.* [20] used parameters according to ASHRAE norm [34], only the optical efficiency is comparable to η_0 of ISO norm. All the results are qualitatively close. One can only notice a decrease of η_0 much more significant, which can indicate a more pronounced fin effect of the solar collector used for the present simulations than for the other cases.

Tab. 5. Comparison of efficiency coefficients of the present study with literature for the withoutFEP and withoutCovers cases.

	Present study		(Bellos *et al.*, 2015) [20]		Measures for validation	
	withoutFEP	*withoutCovers*	*withoutFEP*	*withoutCovers*	*withoutFEP*	*withoutCovers*
η_0	0.792	0.647	0.7453	0.7536	0.81	0.77
$\Delta\eta_0$		-0.15		0.01		-0.04
a_1	2.93	13.21			3.77	12.31
Δa_1		10.28				8.54
a_2	0.007	0.001			0.013	0.013
Δa_2		-0.006				0

Our results also allow a more precise understanding on how this type of faults should be modelled. Two approaches have been considered in previous works. De Keizer *et al.* [13] assume only an increase of η_0. This assumption is clearly on contradiction of our results, since η_0 actually decreases in some cases and also since the increase of the thermal losses cannot be taken into account. Kalogirou *et al.* [11] propose a modification of the collector efficiency factor F', which amounts to multiplying all three coefficient by the same ratio [22]. This is also not the case in our results, with significant differences between coefficients. It is thus clear that a finer modelling of faults on the transparent cover is required.

5.2 « OPACIFICATION » FAULT

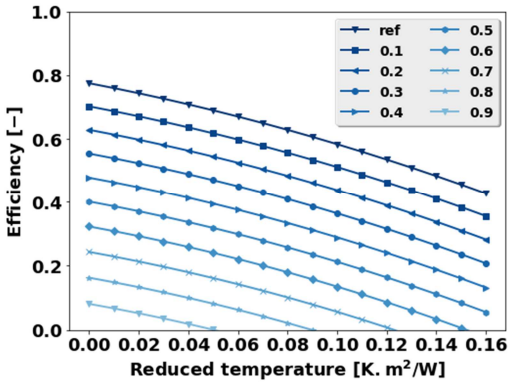

Fig. 8. Efficiency curves of a single collector function of the severity of the « opacification » fault for a direct solar radiation of 1000 W/m² (no diffuse radiation).

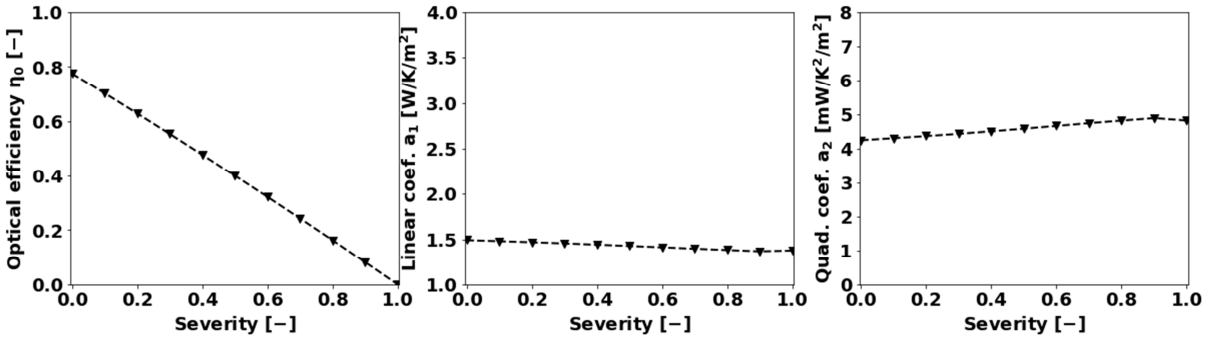

Fig. 9. Variation of efficiency coefficients function of the severity of the « opacification » fault.

Fig. 8 and Fig. 9 show the results of the study for various severities of the « opacification » fault. As shown in Fig. 8, the steady-state efficiency evolves with the severity of the fault, i.e. the efficiency curves have the same shape but progressively move down when the severity increases. This is due to the linear decrease of the optical efficiency η_0.Thermal losses coefficients are very slightly varying: one can observe a slight decrease of a_1 and a small increase of a_2 (see Fig. 9). The effect of this fault is therefore almost independent of the operating temperature of the solar collector. The latter results are expected since for that opacification fault, only the optical properties (transmittance) are modified.

In fact, in this case, the mathematical relationship between the optical efficiency and the transmittance factor can be expressed directly using (7):

$$\eta_0 = F'(\tau\alpha) = F' \frac{\tau_{eq}\alpha}{1-(1-\alpha)\rho_{eq}} \tag{7}$$

with α the absorption coefficient of the absorber plate, F' the collector efficiency factor, τ_{eq} and ρ_{eq} respectively the global transmittance and the global reflectance of the cover glass and FEP foil. τ_{eq} is defined by (8).

$$\tau_{eq} = \frac{\tau_c \tau_t}{1-\rho_c \rho_t} \tag{8}$$

Considering that $\rho_v \rho_t \cong 0$, (8) can be approximated by $\tau_{eq} \cong \tau_c \tau_t$ so that (9) is finally obtained.

$$\eta_0(s_{opa}) \sim \frac{(1-s_{opa})\tau_c \tau_t \alpha}{1-(1-\alpha)\rho_{eq}} = (1-s_{opa})\eta_{0,ref} = (1-s_{opa}) \times 0.906 \tag{9}$$

The coefficients of the linear function obtained in (9) are close to the ones obtained by fitting of the η_0 in Fig. 9.

Fig. 10 compares the obtained results concerning optical efficiency coefficient to those of the literature and experimental measures for the validation of the section 4. A main observation is that the results are consistent.

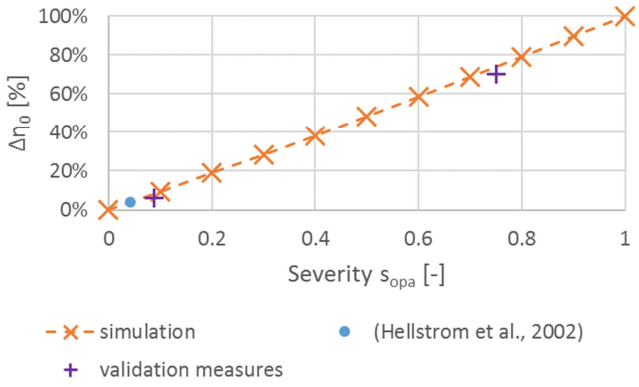

Fig. 10. Comparison of the obtained optical efficiency variations function of the severity of the « opacification » fault with literature and experimental measures used for validation in section 4.3.

Only de Keizer *et al.*[13] proposed a way of modeling the « opacification » fault in previous work. In this case, their proposal is to model this fault by a decrease of the optical efficiency η_0, which is consistent with our results. Additionally, our work shows that this decrease is directly proportional to the severity of the fault and to the amount of reduction of the transmittance of the cover glass (see (5)).

5.3 « INSULATION DEGRADATION » FAULT

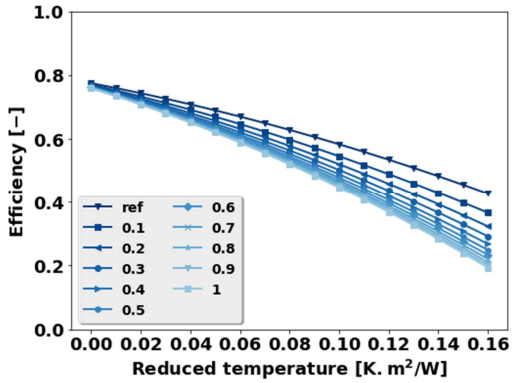

Fig. 11. Efficiency curves of a single collector function of the severity of the « insulation degradation » fault for a direct solar radiation of 1000 W/m² (no diffuse radiation).

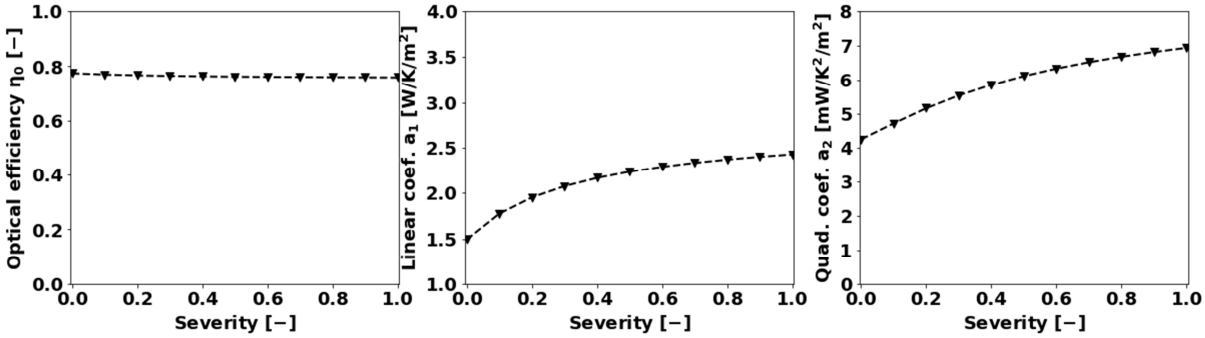

Fig. 12. Variation of efficiency coefficients functions of the severity of the « insulation degradation » fault.

Fig. 11 and Fig. 12 show the results of the study for various severities of the « insulation degradation » fault. This fault does not affect the intercept point of the steady-state efficiency curve of the solar collector, but its slope is increased (see Fig. 11). Concerning the efficiency coefficients (see Fig. 12), the following observations can be done:

- a significant increase of a_1. Conduction exchanges through insulation are in this study modeled by a transfer coefficient independent from temperature. This exchange is therefore directly proportional to the temperature difference between the two faces of the insulation. So its rise naturally modifies the linear coefficient of thermal losses a_1.
- an increase of a_2. This effect was less expected. It can be explained by a rise of the temperature difference between absorber plate and insulation and so an aggravation of the nonlinear losses as infrared radiations or convection through the air space. There is for instance a mean difference temperature of 9.1 K without fault and of 34.3 K with, for an inlet fluid temperature of 60°C.

Experimental measures used for the validation of the model in section 4 gave the same tendencies, but more pronounced since it was an extreme case in which the insulation were totally removed. Results are detailed in Tab. 6.

Tab. 6. Efficiency coefficients obtained with experimental tests of the validation (section 4.3).

	No fault	Without insulation
η_0	0.81	0.80
a_1	3.77	8.56
a_2	0.013	0.036

The results obtained here can be compared to previous work by Vejen *et al.*[21], who tested three different insulation materials. Fig. 13 presents the efficiency curves they obtain, which correspond to the cases on Fig. 11 with severities of 0.7% and 1.5%.

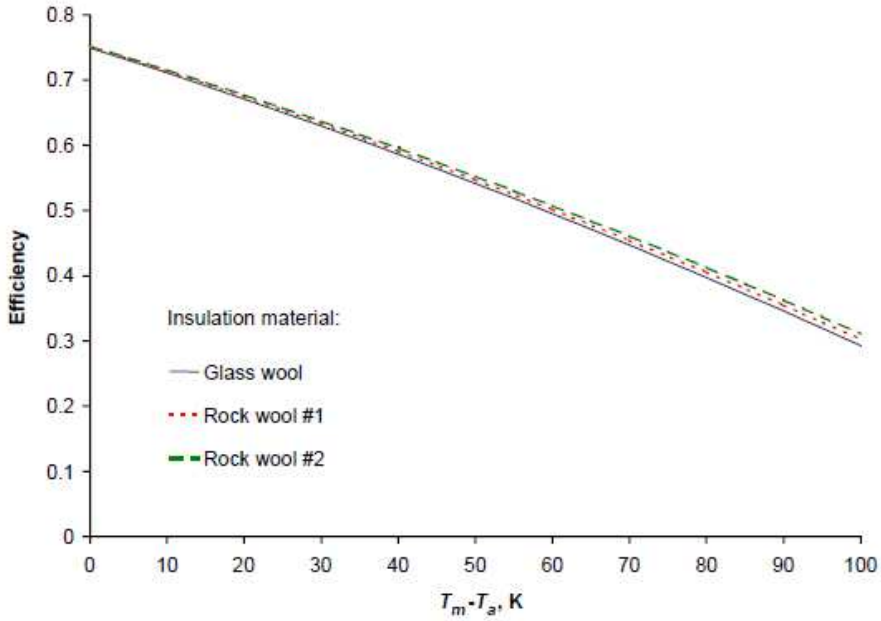

Fig. 13. Efficiency curves of a solar collector function of its insulation material for a solar irradiation of 800 W/m² [21].

The insulation degradation has been modelled in two previous works. De Keizer *et al.* [13] modeled it by an increase of the linear thermal losses coefficient a_1. Lalot *et al.* [35] proposed a slight decrease of F' with a significant rise of the unique thermal losses coefficient U_L. Their model indeed uses the coefficients of the ASHRAE norm [34], which proposes a linear regression of the efficiency curve instead of a quadratic one for the ISO norm. These models seem quite realistic except that they do not take account of the modification of the quadratic thermal losses coefficient a_2. Moreover, the relationship between the increase of the thermal conductivity of the back insulation λ_{isol} (see (6)) and the modification of the efficiency coefficients is not straightforward and requires more work.

6 CONCLUSION

In this paper, the impact of three faults, i.e. « transparent cover failure », « opacification » and « insulation degradation » faults, on the efficiency coefficients of a solar collector for several severity of each fault was analyzed. First, a detailed modular flat-plate solar collector model was developed, which enables a parameterization with physical features. These physical parameters enable a quick, easy and accurate simulation of the three chosen faults. The validation with experimental measures presented in section 4 also demonstrated that the different models are realistic. Moreover, they do not require a calibration of the parameters to be accurate. The last part of this study was dedicated to the use of the different models to assess the link between each fault and efficiency coefficients of the solar collector. The choice of a numerical study enabled us to present results for different severity of each fault and to compare it to the literature. In particular there was a discussion about the modeling choices of the precedent studies, which use efficiency coefficients. We showed that some assumptions can be challenged, while other are validated for a wider range of conditions.

This study also demonstrates that the three analysed faults have a different effect on the efficiency of a flat-plate solar collector. These special modifications of the behaviour of the system are called *signatures* in fault detection and diagnosis area. They are dependant of the extent of the fault, so the Tab. 7 takes and summarizes the results of the section 5 of this paper to derive these signatures and give quantified values for typical extent of each fault. A symbol indicates, for each efficiency coefficient, how its value is affected by each fault. Typical severities of each fault are chosen according to the literature and expert knowledge of the authors:

- The most frequent case of « transparent cover failure » fault is currently the tearing of the FEP film as glazed cover benefits from past experience and normalization.
- A severity of 20% for « opacification » fault corresponds to the decrease of the transmittance factor proposed by Rehman *et al.* [5] as a typical decrease.
- A severity of 20% for « insulation degradation » fault corresponds to a multiplication of the thermal conductivity by 2.5 due to a moisture contents of 5-20% by volume of mineral wool as measured by Jerman *et al.* [30].

The modifications of the efficiency coefficients seem to be high enough to enable a detection of the typical faults. Moreover the final signatures are distinct for each studied fault, which indicates that they could be identified by an appropriate algorithm. Tab. 7 can be the base to construct such an identification method.

Tab. 7. Signature of the three studied faults based on the proposed simulations of this paper and modification of the efficiency coefficients for typical extents of these faults. "↑↑" stands for significant increase, "↑" for a slight increase, "=" for no clear modification, "↓" for a slight decrease and "↓↓" for a significant decrease.

Fault	η_0	a_1	a_2
Transparent cover failure *(withoutFEP)*	= *(+2.3%)*	↑↑ *(+97%)*	↑↑ *(+75%)*
Opacification ($s_{opa} = 0.2$)	↓ *(-19%)*	= *(-1.7%)*	= *(+9%)*
Insulation degradation ($s_{isol} = 0.2$)	= *(-0.9%)*	↑ *(+31%)*	↑ *(+29%)*

Future work will focus on the analysis the sensitivity of the results against measurement uncertainties, specific plant (weather, hydraulic and controlling schemes), other designs of solar collectors, etc. In particular, the influence of the incident angle should be tested. It is then planned to complete this study with other faults and to extend it to a whole solar thermal system. The results will allow the development of an automatic fault identification algorithm which enables a faster repair of the dysfunctions. This algorithm could be based on the development of a machine learning

model of the steady-state efficiency of a solar collector as tested by Esen *et al.*[36] with a least-squares support vector machine for solar air heater.

ACKNOWLEDGEMENT

This project has received support from the French State Program “Investment for the Future” bearing the reference (ANR-10-ITE-0003).

REFERENCES

[1] IEA. Energy and climate change. 2015.
[2] AEBIOM, EGEC, ESTIF. Renewable heat sources: the best available solution to decarbonise the heating sector. 2017.
[3] ISO. EN ISO 9806:2013. Énergie solaire — Capteurs thermiques solaires — Méthodes d’essai. 2014.
[4] Hellstrom B, Adsten M, Nostell P, Karlsson B, Wackelgard E. The impact of optical and thermal properties on the performance of flat plate solar collectors. Renew Energy 2003;28:331–44.
[5] Rehman H ur, Hirvonen J, Sirén K. Influence of technical failures on the performance of an optimized community-size solar heating system in Nordic conditions. J Clean Prod 2018;175:624–40.
[6] Bun L. Détection et localisation de défauts pour un système PV. phdthesis. Université de Grenoble, 2011.
[7] Faure G, Vallée M, Paulus C, Tran QT. Reviewing the dysfunctions of large solar thermal system: a classification of sub-systems reliability. ISES Conf. Proc. 2016, Palma de Mallorca (Spain): 2016.
[8] Cozzini M, Pipiciello M, Fedrizzi R, Hassine IB, Pietruschka D, Söll R. Performance Analysis of a Flat Plate Solar Field for Process Heat. Energy Procedia 2016;91:11–9.
[9] Tagliafico LA, Scarpa F, De Rosa M. Dynamic thermal models and CFD analysis for flat-plate thermal solar collectors – A review. Renew Sustain Energy Rev 2014;30:526–37. doi:10.1016/j.rser.2013.10.023.
[10] Schnieders J. Comparison of the energy yield predictions of stationary and dynamic solar collector models and the models’ accuracy in the description of a vacuum tube collector. Sol Energy 1997;61:179–90. doi:10.1016/S0038-092X(97)00036-4.
[11] Kalogirou S, Lalot S, Florides G, Desmet B. Development of a neural network-based fault diagnostic system for solar thermal applications. Sol Energy 2008;82:164–72. doi:10.1016/j.solener.2007.06.010.
[12] Degelman LO. Calibrated simulation of a solar hot water system to match degraded performance over a 22-year period using two models. Build Environ 2008;43:628–37. doi:10.1016/j.buildenv.2006.06.021.
[13] de Keizer C. Simulation-based long-term fault detection of solar thermal systems. Kassel University, 2012.
[14] Matuska T, Zmrhal V. A mathematical model and design tool - Kolektor 2.2 - Reference handbook 2009.
[15] Zima W, Dziewa P. Modelling of liquid flat-plate solar collector operation in transient states. Proc Inst Mech Eng Part J Power Energy 2011. doi:10.1177/09576509JPE1044.
[16] Hamed M, Snoussi A, Brahim AB. Energy and exergy analysis of flat plate solar collectors in transient behaviors. 2014 5th Int. Renew. Energy Congr. IREC, 2014, p. 1–6. doi:10.1109/IREC.2014.6826943.

[17] Herrero López S, López Perez S, del Hoyo Arce I, Mesonero Dávila I. Dynamic Modelling of a Flat-Plate Solar Collector for Control Purposes, Versailles (France): 2015, p. 419–26. doi:10.3384/ecp15118419.
[18] Kamiński K, Krzyżyński T. Modeling and Simulation of the Solar Collector Using Different Approaches. Mechatron. Ideas Chall. Solut. Appl., Springer, Cham; 2016, p. 131–51. doi:10.1007/978-3-319-26886-6_9.
[19] Bava F, Furbo S. Comparative test of two large solar collectors for solar field application. Proc. EuroSun 2014, 2014.
[20] Bellos E, Tzivanidis C, Korres D, Antonopoulos KA. Thermal analysis of a flat plate collector with Solidworks and determination of convection heat coefficient between water and absorber. ECOS Conf., 2015.
[21] Vejen NK, Furbo S, Shah LJ. Development of 12.5 m2 solar collector panel for solar heating plants. Sol Energy Mater Sol Cells 2004;84:205–23. doi:10.1016/j.solmat.2004.01.037.
[22] Duffie JA, Beckman WA. Chapter 6 : Flat-Plate Collectors. Sol. Eng. Therm. Process. 4 edition, Hoboken: Wiley; 2013.
[23] McAdams WH. Heat transmission. 3rd edition. New York: McGraw-Hill; 1954.
[24] Arnold JN, Catton I, Edwards DK. Experimental Investigation of Natural Convection in Inclined Rectangular Regions of Differing Aspect Ratios. J Heat Transf 1976;98:67–71. doi:10.1115/1.3450472.
[25] Shah RK, London AL. Laminar flow forced convection in ducts: a source book for compact heat exchanger analytical data. Academic Press; 1978.
[26] Colburn AP. Trans AIChE 1933;29:174.
[27] Faure G. Etude de défauts critiques des installations solaires thermiques de grande dimension : définition, modélisation et diagnostic. Communauté Université Grenoble Alpes, 2018.
[28] Peuser F-A, Remmers K-H, Schnauss M. Installations solaires thermiques : Conception et mise en oeuvre. Berlin, Allemagne : Paris: Le Moniteur Editions; 2005.
[29] Isermann R. Fault-Diagnosis Systems - An Introduction from Fault Detection to Fault Tolerance. 2006.
[30] Jerman M, Černý R. Effect of moisture content on heat and moisture transport and storage properties of thermal insulation materials. Energy Build 2012;53:39–46. doi:10.1016/j.enbuild.2012.07.002.
[31] Antepara I, PavlíK Z, žUmáR J, PavlíKová M, čErný R. Properties of Hydrophilic Mineral Wool for Desalination of Historical Masonry. Mater Sci 2016;22. doi:10.5755/j01.ms.22.1.7333.
[32] CSTB. Avis Technique 14/13-1891 - WTS F1 – type K1. 2014.
[33] Bava F, Furbo S, Perers B. Simulation of a solar collector array consisting of two types of solar collectors, with and without convection barrier. Energy Procedia 2015.
[34] ASHRAE. Standard 93-2010 -- Methods of Testing to Determine the Thermal Performance of Solar Collectors. 2010.
[35] Lalot S, Kalogirou S, Desmet B, Florides G. Fault diagnostic method for a water heating system based on continuous model assessment and adaptation. Proc. Eurosun 2008, Lisbonne, Portugal: 2008.
[36] Esen H, Ozgen F, Esen M, Sengur A. Modelling of a new solar air heater through least-squares support vector machines. Expert Syst Appl 2009;36:10673–82. doi:10.1016/j.eswa.2009.02.045.